Journal of the European Ceramic Society **8** (1991) 3–9

Formation of an Y/Ce-Doped α-Sialon Phase

Thommy Ekström,[a] Kjell Jansson,[a] Per-Olof Olsson[b] & Jonas Persson[a]

[a] Department of Inorganic Chemistry, University of Stockholm, S-106 91 Stockholm, Sweden
[b] National Defense Research Establishment, S-172 90 Sundbyberg, Sweden

(Received 17 January 1991; accepted 30 January 1991)

Abstract

α–β-Sialon materials were prepared with a constant molar addition of $Y_2O_3 + CeO_2$ sintering aid with varied composition: 0, 25, 50, 75 and 100 mol% Y_2O_3. The α-sialon grains formed in the microstructure were carefully investigated by analytical and high-resolution electron microscopy. It was found that the α-sialon structure can accept a small amount of cerium to enter the large interstitial cages, if it is stabilized by simultaneous additions of yttrium. Extended crystal defects were found to occur in the α-phase framework; this has not been observed with only yttrium added.

Es wurden α–β-Sialonwerkstoffe hergestellt, denen als Sinterhilfsmittel ein jeweils konstant gehaltener Anteil $Y_2O_3 + CeO_2$ zugesetzt wurde. Das Verhältnis von Y_2O_3 und CeO_2 wurde zwischen 0, 25, 50, 75 und 100 mol% Y_2O_3 variiert. Die α-Sialonkörner des Gefüges wurden mittels analytischer und hochauflösender Elektronenmikroskopie sorgfältig untersucht. Es hat sich gezeigt, daß die α-Sialonstruktur geringe Mengen an Cer auf Zwischengitterplätzen aufnehmen kann, wenn sie durch die parallele Zugabe von Yttrium stabilisiert wird. In der α-Phase konnte eine große Anzahl von Kristallfehlern nachgewiesen werden, die bei alleiniger Yttriumzugabe nicht auftraten.

On a préparé des matériaux sialon α–β possèdant une teneur molaire constante en ajouts de frittage $Y_2O_3 + CeO_2$ ayant les compositions suivantes: 0, 25, 50, 75 et 100% molaires de Y_2O_3. Les grains de sialon α formés dans la microstructure ont été étudiés attentivement par microscopie électronique analytique et à haute résolution. On a établi que la structure du sialon α pouvait accepter une faible quantité de cérium pénétrant dans les cages intersticielles de grande dimension, lorsqu'il est stabilisé par des additions simultanées d'yttrium. Des défauts cristallins de taille importante ont été observés dans le réseau de la phase α; ils n'ont pas été trouvés dans le cas de l'addition d'yttrium seul.

1 Introduction

The α-sialon phase, isostructural with α-Si_3N_4, has a solid solution range described by the general formula $Me_mSi_{12-(pm+n)}Al_{(pm+n)}O_nN_{16-n}$ for a metal ion Me^{p+}. Two mechanisms act simultaneously, giving this solid solution phase a two-dimensional extension in the plane Si_3N_4–MeN. 3AlN–4/3(AlN . Al_2O_3) of a five-component Me–Si–Al–O–N system. The first substitution mechanism is similar to that found for β-sialon, with n(Si + N) being replaced by n(Al + O), and thus does not change the overall electron balance. The second mechanism is a further replacement of pmSi^{4+} by pmAl^{3+}, and the valency change introduced by this substitution is compensated by m metal ions Me^{p+} being incorporated into the large interstitial sites of the α structure. The elements Me that have been found to stabilize α-sialon are Li, Mg, Ca, Y and the lanthanoids with the exception of La, Ce, Pr and Eu.[1–4] Thus the largest Me^{p+} ion in the lanthanoid series which has been reported to enter the α-sialon structure is Nd^{3+}, with an ionic radius around 0·10 nm.[5]

The oxides CeO_2 and Ce_2O_3 have been used successfully as sintering aids for silicon nitride[6–13] or sialon ceramics,[14,15] and the phases formed in the Ce–Si–Al–O–N system are very similar to those found in the well-known Y–Si–Al–O–N system.[16,17] As mentioned previously, additions of cerium oxide to sialon ceramics prior to sintering will not stabilize the α-sialon phase, and in these materials consequently only β-Si_3N_4 or β-sialon will be found. Studies by Söderlund & Ekström[15] on pressureless sintering of sialon ceramics with additions of Y_2O_3 and CeO_2 confirm that Y but not Ce forms the α-sialon phase.

However, if they are added together some observations indicate the presence of a small amount of cerium in the α-sialon phase. This has also been noted in a high-resolution electron microscopy study by Olsson[14,18] on α–β-sialon materials sintered with simultaneous addition of Y_2O_3 and CeO_2 (in the ratio 1/3). It was also found that the α-sialon grains formed were unusually rich in defects, indicating a special tendency for the presence of cerium to initiate defects in the lattice.

A possible mechanism for the inclusion of cerium in the α-sialon structure might be that the smaller Ce^{4+} ion, with an ionic radius of 0·080 nm, to some extent enters the α-sialon structure together with Y^{3+} ($r = 0{\cdot}089$ nm) during the first stage of sintering and subsequently transforms at higher temperatures to Ce^{3+} with a larger ionic radius of 0·103 nm. This makes the instability of the Ce^{4+} ion important, and it has been reported that CeO_2 transforms to trivalent cerium at temperatures above 1230°C when silicon nitride is present.[19]

To investigate the consequences of Ce addition for the α-sialon formation in more detail, an additional study by analytical electron microscopy, high-resolution electron microscopy and X-ray diffraction was initiated on specimens prepared by hot isostatic pressing (HIP), as well as thermal gravimetry studies of the thermal stability of CeO_2 in a mixture with and without Si_3N_4. The results of this study are now reported.

2 Experimental

The overall composition of the starting powder was Si_3N_4 (H.C. Starck, Berlin, grade LC1) with additions of 0·5 wt% Al_2O_3 (Alcoa, grade A16SG), 9·8 wt% AlN (H. C. Starck, Berlin, grade A) and 6·0–9·25 wt% sintering aid. The latter was a mixture of Y_2O_3 (H. C. Starck, Berlin, 99·9%) and CeO_2 (H. C. Stark, Berlin, chemical grade) giving a constant molar concentration of (Y + Ce) and mole ratios of yttrium to cerium equal to 100/0, 75/25, 50/50, 25/75 and 0/100. For pure Y_2O_3 and pure CeO_2 the amount of sintering aid corresponds to 6·0 wt% and 9·25 wt%, respectively. Compacts of the powder mixture were prepared as described in Ref. 15.

The samples were glass encapsulated and hot isostatically pressed at 1700 and 1825°C for 2 h with 200 MPa of argon. The sintered materials were characterized using the following techniques. The phase analysis was based on X-ray powder diffractograms recorded with Guinier–Hägg focusing cameras working with Cu radiation and using Si as internal standard. The obtained powder photographs were evaluated with a computerized scanner system.[20] For determining the ratio of α- and β-Si_3N_4 or sialon the integrated intensities of the (102) and (210) peaks of the α-phase and the (101) and (210) peaks of the β-phase were used.[21]

The thermal stabilities of the CeO_2 and the CeO_2/Si_3N_4 mixture were investigated by thermal gravimetry, using a Setaram TAG24 set-up. Samples were placed in an Al_2O_3 crucible, and the measurements were preformed in an atmosphere of nitrogen gas. TG thermograms were obtained in the temperature range 800–1500°C with a heating rate of 10 K/min.

Scanning electron microscopy was performed on carbon-coated materials, using a Jeol JSM 820 or Jeol JSM 880 instrument equipped with a Link AN 10 000 EDS analyser. Phase contents were evaluated by analysing the shading in SEM micrographs (7 kV, back-scatter mode) with a Kontron IBAS/IPS image processing system on-line with the Jeol JSM 880. For each sample ten micrographs were used at a magnification of × 8000. Selected specimens were studied in an analytical transmission electron microscope, Jeol 2000 FX. The high-resolution electron microscopy studies were performed on a Jeol 200 CX equipped with a top entry goniometer stage with a possible tilt of ± 10° about two axes. The point-to-point resolution of the microscope is about 0·25 nm.

3 Results

The thermogravimetric study was made on pure CeO_2 and on a mixture of CeO_2/Si_3N_4 in the weight ratio 1/2. It was found that pure CeO_2 was stable up to 1500°C, where it started to decompose. A redox reaction takes place very readily in the mixture of cerium dioxide with silicon nitride, however, in which Ce^{4+} reduces completely to Ce^{3+} at a temperature of 1370°C (see Fig. 1). The subsequent X-ray diffraction analysis of the reaction products showed that they consisted of $Ce_5Si_3O_{12}N$ and small amounts of Ce_2O_3 in unreacted Si_3N_4. The observed weight changes were in accordance with a

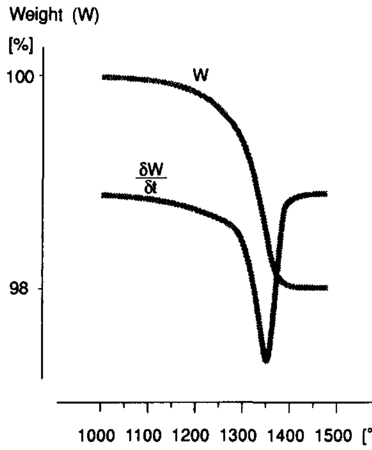

Fig. 1. TG thermogram obtained for a mixture of CeO_2/Si_3N_4, using a heating rate of 10 K/min.

general reaction that can be written as:

$$Si_3N_4 + 9CeO_2 \rightarrow Ce_5Si_3O_{12}N + 2Ce_2O_3 + 3/2\,N_2(g)$$

The starting silicon nitride material consisted of 95% α-Si_3N_4 and 5% β-Si_3N_4, which should convert to α- or β-sialon through a liquid-phase sintering mechanism, at the high temperatures used in this study. As evident from the XRD study of the sintered samples, this had taken place in the specimens at 1700°C with the major part of the added sintering aid being Y_2O_3, and in all specimens at the higher temperature 1825°C. For the other 1700°C samples, with a dominant amount of CeO_2, small amounts of unreacted α-Si_3N_4 could be seen (Table 1). It was therefore decided to use only the 1825°C samples in the electron microscopy study, since these would be closer to equilibrium and since the analysis of the element distribution in the microstructure could be assumed to be simplified by a larger grain size.

It can be noted from Table 1 that the amount of crystalline α-sialon observed by X-ray diffraction in the 1825°C preparation increases when 25% of the added Y_2O_3 is replaced by the same amount of CeO_2 in the 75/25 specimen. Since this method does not detect amorphous phases, and thus the increase in the α/β ratio for small additions of CeO_2 might not be absolute, a complementary study was made on SEM micrographs to verify this observation and to quantify the amount of the glassy phase. Micrographs obtained in the back-scatter mode at an acceleration voltage of 7 kV were used. Thus only information from the surface zone was obtained and the contribution from the bulk was minimized. The investigated specimens were 100/0, 75/25 and 50/50, and a representative micrograph of the 75/25 specimen is shown in Fig. 2. The phases present appear in different shades of grey levels according to the mean atomic number of the atoms within each phase. Thus, β-sialon grains appears dark, α-sialon grains are grey and the Y/Ce-rich intergranual glassy phase shows a white contrast. The shading was analysed on ten micrographs of each specimen. The obtained amounts (vol.%) of the different phases are summarized in Table 2. The analysis showed the volume fraction of glassy phase to be almost constant in all samples at about 3–4 vol.%. However, when comparing these results with the XRD phase analysis, the latter generally seems to give a higher concentration of α-sialon phase than the image analysis. This is due to the choice of limits for the grey levels associated with each phase present, and the major problem is to distinguish the shade of thin β-sialon grains with some glassy phase behind from that of α-grains. However, a good correlation of the general trend of the α-sialon concentrations in different specimens is found. In particular, the increase in α-content for the 75/25 sample compared to that of 100/0 is verified.

To tentatively describe the overall composition of a large number of α-sialon grains, a point analysis of separate grains was performed, by EDS in SEM at 15 kV accelerating voltage, of the Y/Ce = 75/25 and 50/50 specimens. Since the resolution of the probe in this case is about 1 μm, and as the grain size is of the order 2–5 μm, spurious contributions from the surrounding glassy phase or from other grains were occasionally obtained and it is therefore difficult to

Table 1. Phase contents (vol.%) obtained from X-ray diffraction analysis of the samples HIP-ed at 1700 and 1825°C for 2 h

Y/Ce ratio	*1700°C*			*1825°C*	
	α-Si_3N_4	*α-Sialon*	*β-Sialon*	*α-Sialon*	*β-Sialon*
100/0	—	39	61	38	62
75/25	—	27	73	50	50
50/50	4	18	78	41	59
25/75	2	22	76	28	72
0/100	7	—	93	—	100

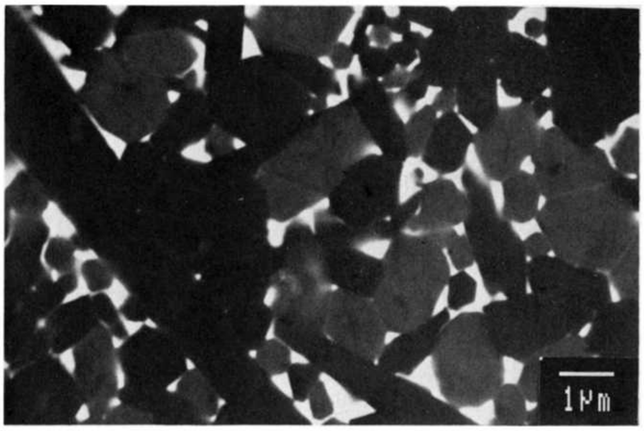

Fig. 2. SEM micrograph obtained in back-scatter mode for the sample with Y/Ce = 75/25.

Table 2. Analysis of the phase contents in specimens prepared at 1825°C

Y/Ce ratio	*α-Sialon (vol.%)*	*β-Sialon (vol.%)*	*Glassy phase (vol.%)*
100/0	44 ± 6	53 ± 6	3 ± 1
75/25	65 ± 9	35 ± 9	4 ± 1
50/50	39 ± 4	58 ± 4	4 ± 1

An image processing system was used to evaluate back-scattered SEM micrographs. The given values represent averages of ten different micrographs from each specimen at a magnification of × 8000.

draw any decisive conclusions concerning the exact composition of the individual grains. However, it was found that the α-sialon contained both Y and Ce and, further, that the relative amount of cerium in the α-sialon grains was much smaller than in the added sintering aid mixture.

To quantify these observations a more careful study was made by analytical transmission electron microscopy on very thin specimens. By this method the problem of interfering glassy phase (rich in Y and Ce) due to poor resolution is eliminated, since distinct single grains identified as α- or β-sialon can be analysed. The results obtained from the 75/25 specimen showed, as expected, no Ce (or Y) in the β-sialon grains, but a clear signal for Ce and Y from the α-sialon grains. The results given as mean values of repeated measurements on three different α-sialon grains are summarized in Table 3. The Y/Ce ratio in the α-sialon grains is 10/1 which can be compared with the added 3/1 ratio. Thus a clear redistribution of the Ce ion between the glassy phase and the α-sialon phase occurs, similar to that indicated by the SEM–EDS study reported above. In addition to the Ce and Y content, the elements Si and Al were also determined, showing the Si/Al compositions of the different α-grains to be almost identical. Thus the composition of the α-sialon phase from the analytical results can be summarized by the formula $(Y_{0\cdot9}Ce_{0\cdot1})_{0\cdot33}Si_{10\cdot4}Al_{1\cdot6}O_{0\cdot6}N_{15\cdot4}$ if the amounts of oxygen and nitrogen are calculated from a charge balance.

High-resolution electron microscopy studies were performed on the 1825°C sample having the Y/Ce ratio equal to 75/25. The result showed that various types of defects had formed in the crystal lattice of the α-grains. Many of the defects observed here have been previously reported by Olsson.[14,18] However, an additional type of defect not previously reported was also found, see Fig. 3. The defects are two-dimensional and occupy an approximate crystal area of 750 nm^2, in which the crystal lattice is shifted relative to the main crystal lattice. An example of this kind of defect at a larger magnification is seen in Fig. 4. The defect consists of three different parts, A, B and C. Part A can be related to a type of defect which is formed by a translation of the lattice through approximately one-third of the *c*-axis along the (100) direction,[14] see Fig. 5. The translation of the lattice along the *c*-direction is interrupted in part B, where the border between the undistorted crystal and the defect forms a saw-tooth pattern by alternating between the (100) and (101) directions. Finally, the distortion of the lattice is relaxed in part C by two successive gradual translations along the (100) direction, each equal to approximately one-third of the length of the *c*-axis. The net effect of these translations cancels the shift between the undistorted areas on either side of the defect zone.

Table 3. Analysis of three different distinct α-sialon grains in the specimen with the added molar ratio Y/Ce = 75/25, HIP-ed at 1825°C for 2 h.

	Results (in at %)			
	Si	*Al*	*Y*	*Ce*
Grain 1	83·5	12·5	2·2	0·24
Grain 2	82·9	12·9	2·4	0·26
Grain 3	83·7	12·0	2·5	0·23
Average	83·4	12·5	2·4	0·24

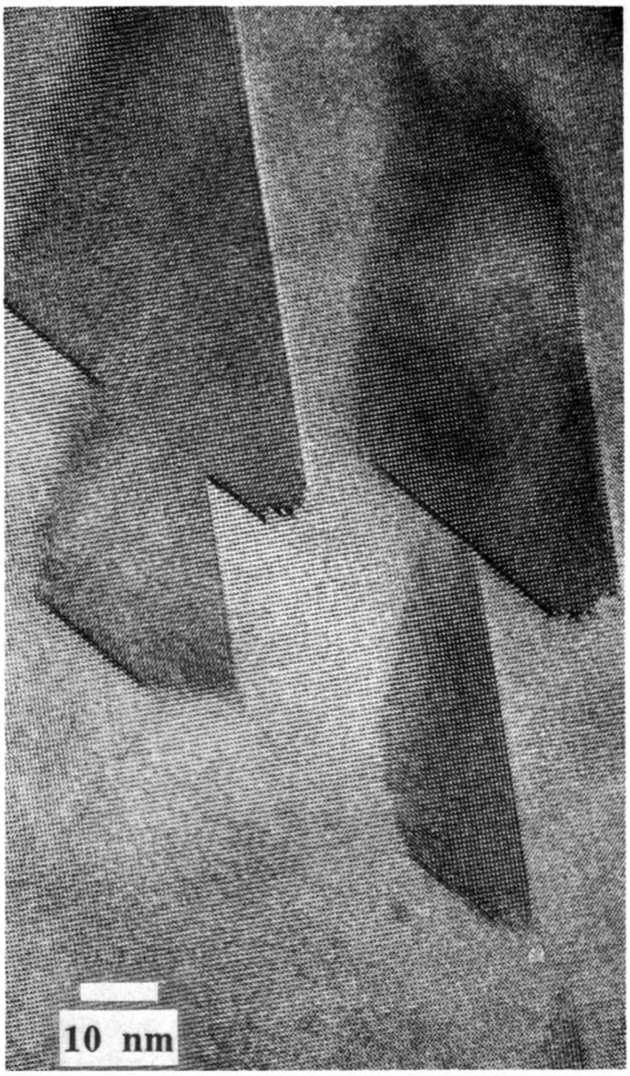

Fig. 3. An (010) image of an α-sialon containing a number of complicated intergrown defects.

4 Discussion

It has been assumed that Nd^{3+}, with an ion radius of about 0·10 nm, is the largest ion able to enter the α-sialon structure.[5] Yttrium, with an ion radius (in 6-coordination) around 0·089 nm, thus has no difficulty in entering an α-sialon structure and neither should Ce^{4+}, with a size around 0·080 nm. However, the result of the thermogravimetric analysis made in this study confirmed the previous information that CeO_2 is unstable in mixtures with Si_3N_4. It was found in this study that, at temperatures above 1370°C, CeO_2 will transform completely to the Ce^{3+}-compounds Ce_2O_3 and $Ce_5Si_3O_{12}N$, and nitrogen gas will be released. The ion size of Ce^{3+}, stable at the sintering temperatures, is 0·103 nm,

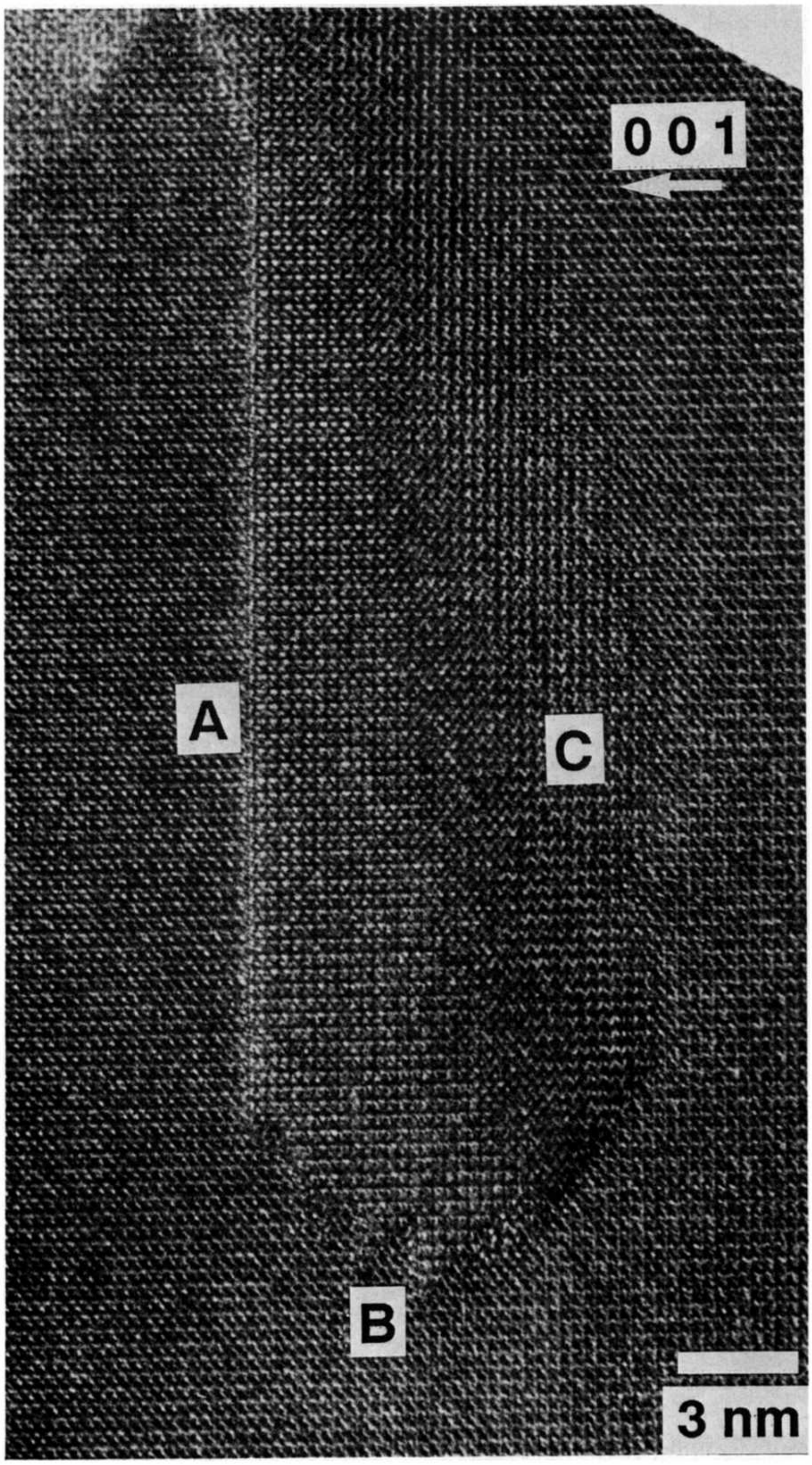

Fig. 4. An (010) image of an α-sialon crystal, showing an example of a type of crystal defect commonly found in the investigated sample. The labels A, B and C mark the different parts of the defect discussed in the text.

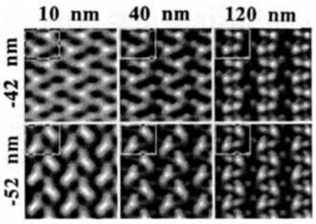

Fig. 5. Calculated (010) images of the hexagonal α-sialon structure ($a = 0{\cdot}762$ nm and $c = 0{\cdot}568$ nm) for two different focuses (−42 nm and −52 nm) and three different crystal thicknesses (4, 12 and 20 nm). The projected unit cell is indicated in each image.

which is slightly larger than the size of Nd^{3+}. Thus Ce^{3+} alone would not be able to enter the α-sialon structure.

The lower compositional limit of the Y-containing α-sialon phase, $Me_mSi_{12-(3m+n)}Al_{(3m+n)}O_nN_{16-n}$, has been reported as 0·3,[1] 0·33,[22,23] 0·34[24] and 0·40 ± 0·05.[25] For Nd the limit is 0·33[24,25] and for other rare earth metals the range 0·33–0·36 has been reported.[24] The observed value of around $m = 0{\cdot}33$ for the (Y + Ce) incorporation into the α-sialon phase in this study is thus very close to previous reports on the lowest solubility limit.

The relative amount of cerium found in the (Ce + Y)-stabilized α-sialon phase is much lower than the relative cerium amount in the added (Ce + Y)–metal oxide mixture. This indicates that cerium does not easily enter into the interstitial holes in the α-sialon structure, even if another smaller metal ion like yttrium stabilizes the structure. The presence of cerium in the α-sialon structure can hypothetically have different causes. One possibility is, as mentioned above, that it enters in an early stage of the sintering as the Ce^{4+} ion. Once present in the structure it would transform to Ce^{3+}, stable at high temperatures, and thus, because of its size, it would be trapped in the framework. The results of the present study show, however, that this is not the case, since most of the α-sialon phase will not crystallize from the sintering liquid until the added silicon and aluminium nitrides start to dissolve in more substantial amounts at temperatures above about 1700°C. No Ce^{4+} would be present at these high temperatures, since CeO_2 in the presence of an excess amount of silicon nitride rapidly transforms at much lower temperatures.

Another possible reason is that only yttrium is able to stabilize the α-sialon structure and, once the α-sialon phase is formed, small amounts of Ce^{3+} are able to enter the structure. This latter reaction path also implies that in other similar Me–Si–Al–O–N systems, where a smaller Me ion is able to stabilize the α-sialon structure, a simultaneous addition of cerium would create a similar situation with some small part of cerium entering the α-sialon structure.

One possible reason for this behaviour of the Ce^{3+} ion can be seen from the relative sizes of different rare earth ions plotted against the amount of α-sialon formed in Fig. 6. The very same overall composition was used to prepare an α–β-sialon ceramic with the use of different metal oxide additives.[26] The relative ion size is seen to have a significant effect on the amount of α-sialon formed. It is also seen that Ce^{3+} size is very close to the upper ion size limit able to stabilize the α-sialon structure. The still larger ion La^{3+}, with $r = 0{\cdot}108$ nm, has been shown in previous studies to be unable to enter α-sialon even in combination with added yttrium.[27,28]

The sample chosen for the high-resolution TEM had a Y/Ce ratio of 75/25 and contained a high concentration of α-phase. It differs from the samples previously investigated by Olsson,[14,18] which contained sintering aid additions with a Y/Ce ratio equal to 25/75 and thus the question was if the same type and number of defects would occur also in samples with a lower concentration of ceria. It was observed that defects occurred in the 75/25 specimen of various types similar to those found in the 25/75 specimen. A new type of defect not previously reported was also observed. Neither of these defects is found in the pure Y-doped sialons, and it is plausible to suggest that the inclusion of the Ce ions initiates the defects. A possible explanation for this kind of separated defect is that it is formed due to a non-uniform distribution of Ce atoms in the crystals, and thus Ce-rich areas would preferably contain this type of distortion.

In summary it has been shown that the α-sialon structure can accept a small amount of cerium in the large interstitial holes if the structure is stabilized by simultaneously added yttrium. The presence of cerium in the α-sialon grains caused a clearly increased defect population in the crystal lattice.

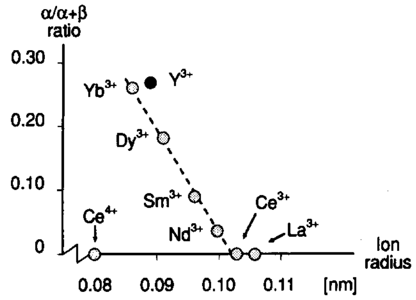

Fig. 6. The concentration of α-sialon formed in α–β-sialon materials of the same overall composition and heat treatment, where yttrium has been replaced by the same amount of rare earth elements with different ion radii (in 6-coordination).[26] Yttrium is also included in the figure for comparison, although it does not belong to the rare earth series.

Acknowledgements

AB Sandvik Hard Materials is thanked for permission to publish the results presented in this article. The work has been financed in part by the National Swedish Board for Technical Development.

References

1. Hampshire, S., Park, H. K., Thompson, D. P. & Jack, K. H., α′-Sialon ceramics. *Nature*, **274** (1978) 880–3.
2. Park, H. K., Thompson, D. P. & Jack, K. H., α′-Sialon ceramics. *Sci. Ceram.*, **10** (1980) 251–6.
3. Stutz, D., Greil, P. & Petzow, G., Two-dimensional solid-solution formation of Y-containing α-Si_3N_4. *J. Mater. Sci. Letters*, **5** (1986) 335–6.
4. Slasor, S. & Thompson, D. P., Comments on two-dimensional solid-solution formation of Y-containing α-Si_3N_4. *J. Mater. Sci. Letters*, **6** (1987) 315–6.
5. Slasor, S., Liddell, K. & Thompson, D. P., The role of Nd_2O_3 as an additive in the formation of α′- and β′-sialon. *Brit. Ceram. Proc.*, **37** (1986) 51–64.
6. Huseby, I. C. & Petzow, G., Influence of various densifying additives on hot-pressed Si_3N_4. *Powder Met. Int.*, **6** (1974) 17–19.
7. Mah, T.-I., Mazdiyasni, K. S. & Ruh, R., The role of cerium orthosilicate in the densification of Si_3N_4. *J. Am. Ceram. Soc.*, **72** (1979) 12–16.
8. Mah, T.-I., Mazdiyasni, K. S. & Ruh, R., Characterization and properties of hot-pressed Si_3N_4 with alkoxy-derived CeO_2 or Y_2O_3 as sintering aids. *Am. Ceram. Soc. Bull.*, **58** (1979) 840–4.
9. Sanders, W. A. & Mieskowski, D. M., Strength and microstructure of sintered Si_3N_4 with rare-earth-oxide additions. *Am. Ceram. Soc. Bull.*, **64** (1985) 304–9.
10. Tani, E., Umebayashi, S., Kishi, K., Kobayashi, K. & Nishijima, M., Gas-pressure sintering of Si_3N_4 with concurrent additions of Al_2O_3 and 5 wt% rare earth oxide: High fracture toughness Si_3N_4 with fiber-like structure. *Am. Ceram. Soc. Bull.*, **65** (1986) 1311–15.
11. Hirosaki, N., Okada, A. & Matoba, K., Sintering of Si_3N_4 with the additions of rare earth oxides. *J. Am. Ceram. Soc.*, **71** (1988) C-144–7.
12. Lange, F. F., Si_3N_4–Ce_2O_3–SiO_2 materials: Phase relation and strength. *Am. Ceram. Soc. Bull.*, **59** (1980) 239–40.
13. Arias, A., Effect of CeO_2, MgO and Y_2O_3 additions on the sinterability of a milled Si_3N_4 with 14·5 wt% SiO_2. *J. Mater. Sci.*, **16** (1981) 787–99.
14. Olsson, P.-O., Crystal defects and coherent intergrowth of α- and β-crystals in Y–Ce doped sialon materials. *J. Mater. Sci.*, **24** (1989) 3878–87.
15. Söderlund, E. & Ekström, T., Pressureless sintering of Y_2O_3–CeO_2 doped sialons. *J. Mater. Sci.*, **25** (1990) 4815–21.
16. Jack, K. H., Review: Sialons and related nitrogen ceramics. *J. Mater. Sci.*, **11** (1976) 1135–58.
17. Thompson, D. P., Phase relationships in Y–Si–Al–O–N ceramics. In *Tailoring Multiphase and Composite Ceramics*, ed. R. E. Tressler, G. L. Messing, C. G. Pantano & R. E. Newham. Plenum Press, New York, 1986, pp. 79–91.
18. Olsson, P.-O., High resolution electron microscopy of ceramics: Studies of sialon materials and doped β-rhombohedral boron. Thesis in Chem. Commun. Univ. Stockholm, No. 2, 1989.
19. Jack, K. H., The significance of structure and phase equilibria in the development of silicon nitride and sialon ceramics. *Sci. Ceram.*, **11** (1981) 125–42.
20. Johansson, K.-E., Palm, T. & Werner, P.-E., An automatic microdensitometer for X-ray powder diffraction photographs. *J. Phys.*, **E13** (1980) 1289–91.
21. Käll, P.-O., Quantitative phase analysis of Si_3N_4-based materials. *Chem. Scripta*, **28** (1988) 439–46.
22. Stutz, D., Greil, P. & Petzow, G., Two-dimensional solid-solution formation of Y-containing α-Si_3N_4. *J. Mater. Sci. Letters*, **5** (1986) 335–6.
23. Huang, Z.-K., Greil, P. & Petzow, G., Formation of α-Si_3N_4 solid solutions in the system Si_3N_4–AlN–Y_2O_3. *J. Am. Ceram. Soc.*, **66** (1983) C-96–7.
24. Huang, Z. K., Tien, T. Y. & Yen, T. S., Subsolidus phase relationships in Si_3N_4–AlN–rare earth oxide systems. *J. Am. Ceram. Soc.*, **69** (1986) C-241–2.
25. Käll, P.-O. & Ekström, T., Sialon ceramics made with mixtures of Y_2O_3–Nd_2O_3 as sintering aids. *J. Eur. Ceram. Soc.*, **6** (1990) 119–27.
26. Ekström, T., Liddell, K., Niklewsky, T. & Thompson, D. P., Sintering and properties of Yb, Dy or Sm doped sialons (in press).
27. Ekström, T. & Olsson, P.-O., Pressureless sintering of sialon ceramics with mixed Y_2O_3–La_2O_3 additions. *J. Mater. Sci. Letters*, **8** (1989) 1067–70.
28. Olsson, P.-O. & Ekström, T., HIP-sintered β- and mixed α–β-sialons densified with Y_2O_3 and La_2O_3 additions. *J. Mater. Sci.*, **25** (1990) 1824–32.